

Extreme Terrain Quadruped (ET-Quad)

For Traversing Rocks, Regolith, and Rough Terrain

Team Makeup:

Mechanical Engineering: Derek Vasquez¹ (Lead), Max Austin¹ (Lead), Brian Van Stratum¹, Jason White¹, Hamza Asif^{1,3}, Ashley Chase¹, Jayson Dickinson¹, William Hochstedler¹, David Jay¹, Michael Dina², Cameron Ryals², Andrew Burkhardt², Geraina Johnson², Benjamin Labiner², Dominic Bellocchio², Gissel Reynoso², Jonathan Boylan², Carlos Sanchez-Sarmiento², Francisco Lopez^{2,3}, Dane Seal¹

Electrical Engineering: Zaid Shah^{1,3}, Joseph Lupton¹

Computer Engineering: Justin Cheesborough², Alejandro Chong-Garcia^{2,3}

FAMU-FSU Mechanical Engineering Faculty Advisors

Jonathan
Clark

Christian
Hubicki

Camilo
Ordonez

Shayne
McConomy

Juan
Ordonez

FAMU-FSU College of Engineering
Florida A&M University and Florida State University



Key: 1: Graduate student 2: Undergraduate student 3: Foreign National

1 Quad Chart



Florida State University & Florida A&M University Extreme Terrain Quadruped (ET-Quad) For Traversing Rocks, Regolith, and Rough Terrain



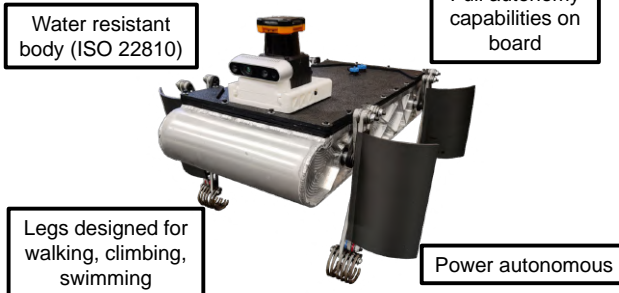
Concept Synopsis

A quadruped robot capable of

- Walking over rough terrain
- Climbing steep (>60 deg) rocky slopes
- Traversing through resistive media

Robot development is based in recent modeling and hardware breakthroughs in climbing and moving through resistive media

Image depicting concept



Innovations

- First legged robot capable of walking, vertical climbing, and swimming
- Multi-modal legs and feet allow walking, climbing, and swimming (resistive media) without hardware changes
- Thermally informed planning allows energy efficient locomotion over lunar orbital cycle
- 3D mapping for multimodal locomotion planning

Verification Testing Results & Conclusions

- Robot is power and control autonomous (no tethers)
- Successful walking up to 25 cm/s
- Climbing capabilities verified
 - Multiple inclines and surfaces
 - Vertical (90 degree) climbing on artificial surface
 - Speeds up to 15 cm/s
- Swimming in water at ~9 cm/s
- Sensors recognize and plan for traversable and non-traversable surfaces
 - Chooses correct gait for locomotion modality (e.g. walk vs. climb)

2 Executive Summary

Extreme Terrain Quadruped (ET-Quad) For Traversing Rocks, Regolith, and Rough Terrain.

Operational Scenario:

The solitary quadrupedal robot slowly makes its way across the lunar landscape, its steps sinking slightly into the layer of regolith coating the ground as it makes its first steps up the edge of the crater wall. Along its journey from the landing site, it has tracked through this barren land measuring, characterizing and, at times, sinking deep into the powdery soil, but always moving forward. Now it faces a new challenge, a rocky patch in its path, nearly vertical. Undaunted, ET-Quad stretches its legs, reorients itself, finds purchase for the spines on its feet, and carefully climbs the crater wall. At the top it will place its sensor and communication payload, the first step of its mission complete.

Proposed Technology Solution:

We propose a small-scale quadrupedal robot with multi-functional legs that allow it to traverse rough terrain, to wade or swim through deep, soft-packed regolith, and to climb up sheer rocky surfaces. On earth, as shown by animals, legs are one of the most versatile and adaptable mechanisms for locomotion on unstructured terrain. Many mammals, including humans, use their appendages to walk, climb, and even swim. The proposed robot is designed based on our recent technological advances in building these multi-modal robots. These include innovations in modeling, leg design, and control.



Figure 1: ET-Quad executing a missions on a crater rim such as mapping, delivering payloads, or characterizing terrain

Verification Testing:

Modeling and simulations have predicted the necessary forces, design features, and control policy for lunar locomotion. The hardware platform built on these results has been verified in walking, climbing, and swimming modalities.

Lunar Exploration Goals:

This type of robot will be able to perform missions relating to:

- Wide area exploration on extreme terrain with energetic constraints
- Deployment of a payload, scanner, or sensor at a geographical location
- Terrain sampling and characterization

Although initially targeting crater exploration on the moon, this technology will also have application to a wide variety NASA missions including lunar base construction and exploration of Mars or asteroids such as 16-Psyche.

3 Problem statement and background

3.1 Mission

Recent studies suggest that some portions of lunar craters, especially those near the poles, may not receive direct solar radiation and may still contain water in the form of ice. Furthermore, the mineral composition, geological formations, and regolith mechanics at the base and edges of craters may yield important information about the early life of the solar system, the earth and the moon. The exploration of crater basins therefore requires deployment of a mobile system capable of navigating uneven terrain. Such a system should be able to navigate steep slopes (by climbing and walking as required), get itself out of fine regolith and move using discrete footholds to navigate the brittle terrain at the base of a crater.

The objective of this project is to demonstrate an alternative lunar mobility solution: a legged robot capable of exploration and delivery of small payloads in unstructured environments such as steep slopes, rocky terrain, and high-porosity regolith.

The proposed quadrupedal robot should be able to demonstrate the following capabilities:

1. Navigate from deployment zone to the edge of a crater or ridge (walking on packed or fluffy regolith),
2. Autonomous foot placement and obstacle negotiation in an energy and power efficient manner,
3. Navigate to and climb 60 degree slopes up to a crater rim,
4. Mapping and characterization of the terrain including surface properties based on ground contact,
5. Deploy and retrieve scientific payload at the base or edge of the crater.

Figure 2 shows aspects of the how these capabilities enable the mission objective.

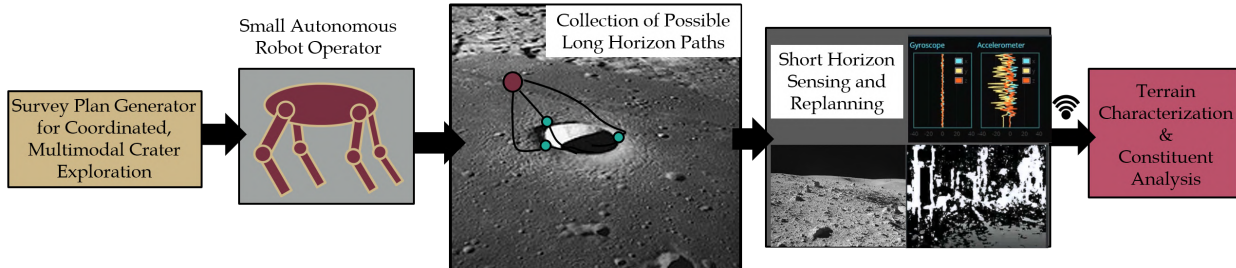


Figure 2: Robot mission for lunar crater exploration and sensory feedback by small robot operator capable of walking, climbing, and traversing resistive terrain (soft regolith).

3.2 Background

From the early successes of humans landing on the moon to the recent exploration of Mars with wheeled, and now rotoed, robots, NASA has a proud history of successful exploration missions. Although much closer than Mars, the exploration of some scientifically interesting locations on the moon presents particular challenges. The lack of an appreciable atmosphere, regions of deep and softly packed regolith, and craters with slopes greater than 30 degrees all work against current designs. Legged robots, such as Lemur, that use gecko-inspired microspines for substrate attachment, show great promise [1, 2]. Our proposed platform builds on these ideas and attempts to extend them to regions that contain deep, lightly-packed regolith, as is expected near the edges of craters and the lunar poles where water may be more available.

Challenge 1 — Crater Structure: The lunar surface is marked by a wide variety of craters, from simple geometries like Moltke, to extremely large (85 km wide) craters with well defined rims, peaks, and walls like Tycho.

Based on the information obtained from the Lunar Reconnaissance Orbiter Camera (LROC), crater walls appear to taper with slopes in the range of 25 to 36 degrees. Degradation of craters walls manifested in the

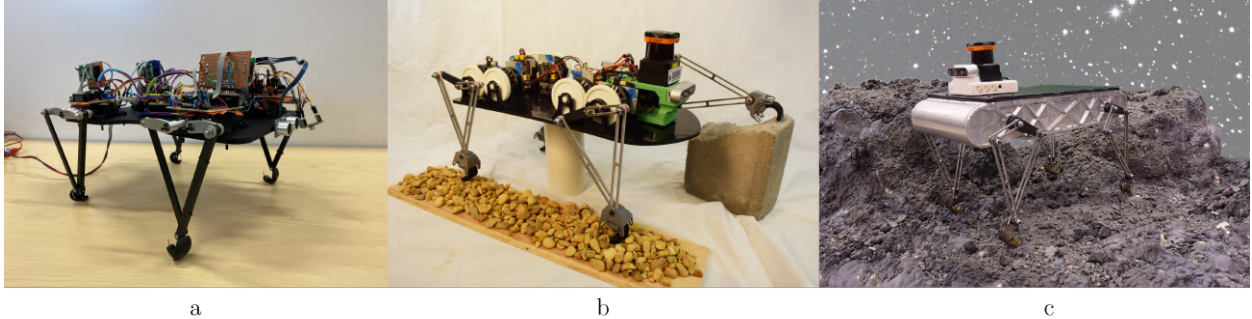


Figure 3: Design progression of the ET-Quad project. a) Initial prototype of ET-Quad prior to receiving funding. b) Preliminary design at the time of the mid-project report. c) Current design of ET-Quad.

form of abrupt local drop-offs area are also likely present [3, 4]. Craters also have limited, and sometimes no direct sunlight, which poses challenges both for energy harvesting and thermal survivability.

Challenge 2 — Loose Regolith: Much of the lunar surface is coated with regolith of varying thickness, often several meters deep [5]. Experts suggest the regolith at the poles may be substantially less dense, due to relative lack of boulders visible at the poles [6]. Mobility through regions of this loose soil is challenging due to reduced traction, terrain deformation, and possible fluidization. Consequently, tracked rovers may get stuck, similar to what happened with the Spirit rover on Mars. Non-conventional methods of locomotion, like swimming, have been proposed for traversal through high-porosity regolith, and improved performance has been demonstrated in tests with regolith simulants [7].

3.3 Overall Approach

The design ideas behind our robot, ET-Quad, are based on our recent advances in developing legged robots. In particular, to overcome these two challenges we combine (1) feet with the directional adhesion properties used by climbing animals and robots such as NASA’s Lemur and our bipedal climber, BOB [8, 9], with (2) limbs and controllers designed for effective movement through deformable, resistive media [10, 11].

Our design approach to build a rover (ET-Quad) capable of moving through these extreme terrains includes:

1. Physics-based simulation for predicting requisite adaptations for lunar travel.
2. Bio-inspired limb design for multimodal movement (rocky slopes, soft regolith, etc.)
3. Control through high-level, sampling-based planners and local methods for fast re-planning and execution.
4. Experimental testing of locomotion strategies.

4 Robot Design Overview

ET-Quad (Figure 3c) is a small-scale quadrupedal robot designed to walk on flat and rough terrain, climb steep slopes up to 90 degrees, and trudge through deep regolith. For Earth development and testing purposes, ET-Quad is also capable of swimming in water which, like loose-packed regolith, we classify as a “resistive media”. Each of these capabilities can be demonstrated on the robot without any changes to the locomotion hardware.

ET-Quad is designed for short-range missions away from a lander or mobile base station to explore difficult to reach crater rims, cliffs, and crevices. We assume the lander or base station is capable of communicating with ET-Quad and Mission Control, as well as providing additional charge to ET-Quad for multiple missions.

This section describes the various subsystems and focuses of the ET-Quad project, including technical specifications and design assumptions. Major changes that have happened since the mid-project report are discussed where appropriate.

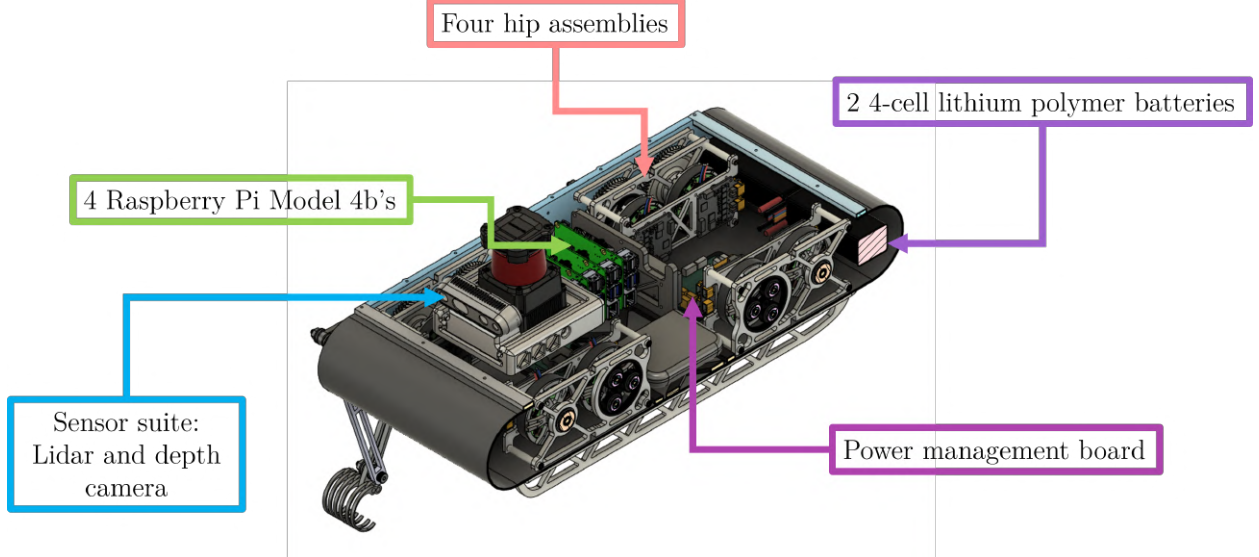


Figure 4: Cutaway CAD view showing the interior layout of ET-Quad. Internal batteries provide power to motors and four Raspberry Pi Model 4b’s, which process sensor data from a depth camera, lidar, and IMU, control motors, and perform onboard mapping and planning functions.

4.1 Hardware Development

ET-Quad walks and climbs using a coaxial and symmetric 5-bar leg mechanism that allows for 2 degree-of-freedom control in each leg. The 5-bar leg was chosen for its mechanical simplicity, proven effectiveness on other legged robots developed at the FAMU-FSU College of Engineering [12], as well as simulation results that suggest that it has near-optimal properties for climbing. Although the two distal links of the 5-bar mechanism do not need to be coaxial, if they are, then the legs can make 360-degree revolutions with no interference.

4.1.1 Motors

ET-Quad is driven by eight brushless DC motors, which have a reported Kv of 330 and peak torque of 1.7 Nm. These are each driven by a mjbots Moteus r4.11 controller. Each leg is operated by two motors, which are assembled as hips inside the body. One motor is attached to a planetary gear set with a 6:1 reduction, while the other is direct drive. The geared motor drives the link that is directed backwards while climbing. This allows for the “elbow” to be close to the substrate and carry most of the weight of the robot when going uphill. The motors and controllers are housed inside the body, and a shaft seal protects against water and dust intrusion.

The motors are driven by two four-cell lithium-ion batteries with a charge of 2800 mAh each, which are housed inside ET-Quad and connected in series. A power distribution board is connected between the batteries and motor controllers, and this board is equipped with current and voltage sensors. These sensors allow ET-Quad to better power consumption and battery life.

4.1.2 Hips

Coaxial output shafts feature two sets of concentric bearings and shaft seals to align the shafts and seal the robot from water at the joint. Having two coaxial output shafts for the legs was the driving force behind the development of the “hip” module. The motors that were chosen to drive the leg have adequate strength to walk, run, and swim, but they lack the torque needed for climbing applications. For this reason, our team decided to implement a 6:1 gear reduction on one of the distal leg links. This asymmetry allows the direct-drive link to be more compliant when absorbing shock, while the geared link provides the torque necessary to pull the robot upward in a climbing gait.

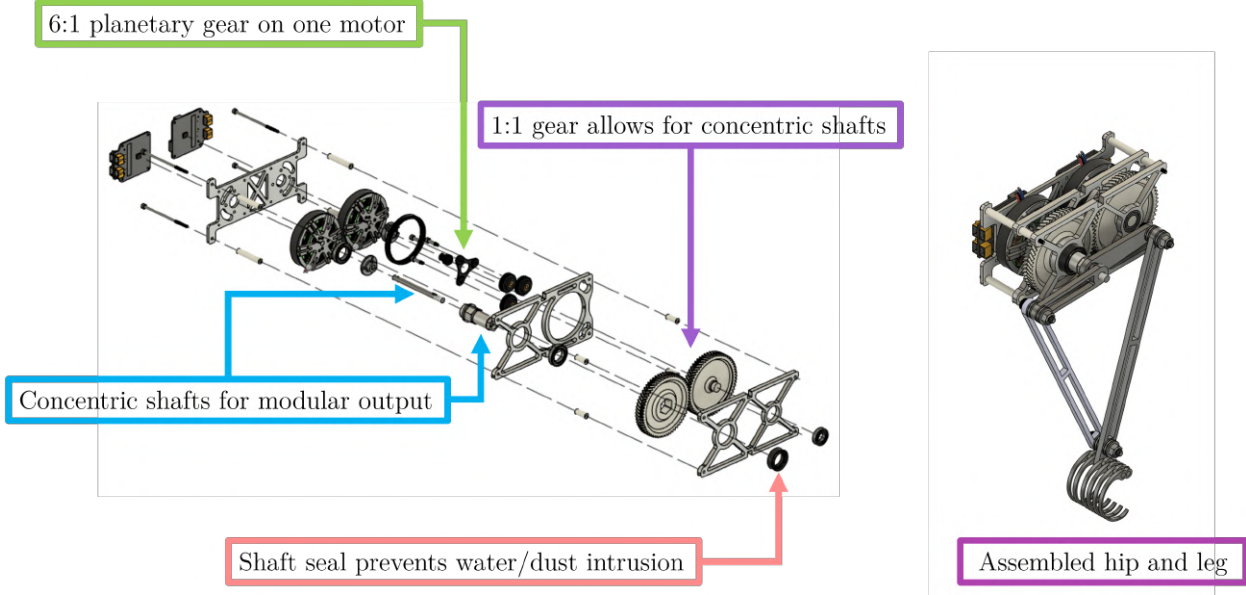


Figure 5: Hip assembly of ET-Quad. One motor directly drives one of the primary links of the 5-bar linkage leg, while another motor is reduced through a 6:1 planetary gear before another 1:1 gear transfers the power to a shaft that is coaxial with the first motor. Also shown is an assembled hip with a leg assembly attached. This assembly is repeated 4 times (two of which are mirrored) on ET-Quad.

The initial hip design was created as a mockup using 3D printed components. This 3D printed hip was created to validate the layout of our gear train, but it was also tested on a boom arm to determine the hip’s strength, power, and its likely failure points. The next version was built from aluminum to allow for a lighter, stronger design, and it also allows the hip module to conduct heat away from the motor drivers and to the side walls of the robot. The CAD design of the hip assembly is shown in Figure 5.

The hip’s modular design reduced assembly errors by having less variance between the assemblies which lowers the Boothroyd-Dewhurst complexity [13], improves the ability to troubleshoot, and improves the efficiencies for assembly times and knowledge transfer.

4.1.3 Legs

The legs used by version 0 were designed using the Dyno-Kinematic Leg Design (DKLD) method [14, 15]. The target dynamics used for the leg design optimization were various SLIP-like [16] bipedal running and walking gaits and Full-Goldman [17] style climbing. The leg design optimization found a successful planar dual-revolute Minitaur [18] style 5-bar linkage which could achieve all of the gait targets under the designer selected and actuator constraints. The 5-bar kinematics were chosen due to their improved actuator work distribution during climbing and relative ease of self-contained fabrication at a small scale.

Dynamic scaling rules [19] were used to morph the leg design for a $1.5 \times$ scale from v0 to that of v1 and v2 of ET-Quad. Further application of these scaling rules was done to validate that the selected actuators would be able to perform under dynamic loads on the both Earth and the moon.

4.1.4 Toes

Legged robots capable of both walking and vertical climbing typically rely on the ability to swap feet that are individually designed for each mode [14, 20]. The design of multimodal feet is complicated by differing compliance requirements for walking and running. Also, a multimodal foot will need to be capable of maintaining sufficient friction while walking and substrate adhesion while climbing. For ET-Quad, we have implemented feet capable of climbing and walking without manual adjustments by assembling each foot as an array of six C-shaped dactyls made of AR500 carbon steel. Each toe is individually compliant and

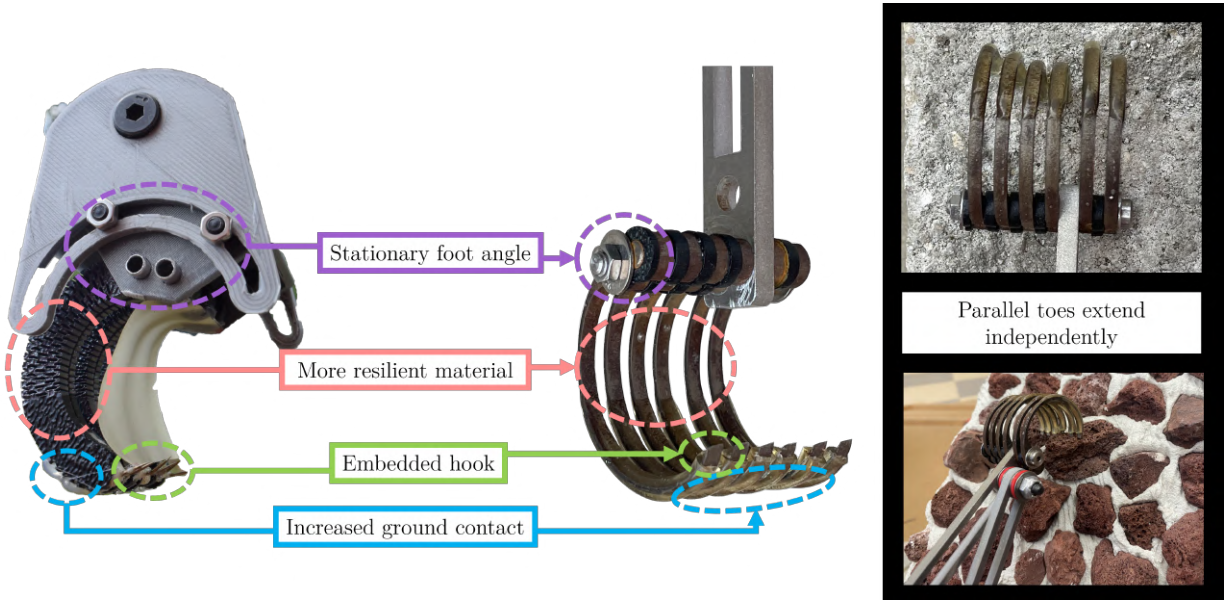


Figure 6: The foot design for ET-Quad has evolved significantly since the Mid-Project Report to improve resilience and minimize weight. The individual dactyls of the foot facilitate robust attachment to varied surfaces.

sharpened to improve attachment to various surfaces. Each toe is also individually dipped in an abrasion resistant rubber to improve traction when walking. This foot design is a significant change from the Mid-Project report, where the toes were made of kufed ABS plastic and the foot had an adjustable angle of attachment. The ABS toes were not strong enough for the forces experienced during locomotion and broke during testing. The adjustable angle of attachment was necessary for testing to discover the best angle for climbing. The new design is fixed at an angle that allows climbing on multiple surfaces.

4.1.5 Swimming

To facilitate locomotion in water as well as loose particulate matter, fins have been fabricated to be attached to the legs. These fins allow for drag based swimming gaits, which generate forward locomotion in water and, we believe, deep regolith. There are currently two prototypes, which have been verified as described in Section 5.2.2. The first is a flap on the inside of the C-shaped feet, which pushes into the feet during a power stroke and moves to allow the flow of water during recovery. The second prototype is a stationary fin that is attached to the secondary links of the 5-bar leg mechanism.

4.1.6 Robot Body

The body of ET-Quad consists of a welded aluminum chassis that holds all locomotion hardware and electronics inside with a lid that is removable for operator access. Shaft seals are press fit into the side which allow for the internal motors to drive the external legs without water intrusion. The lid is held in place by bolts and a rubber gasket prevents water intrusion at the lid interface. Re-sealable ports in the lid allow for battery charging and connection of the sensor suite when ET-Quad is not swimming.

4.2 Sensors and Intelligence

The main computations of ET-Quad take place on a cluster of four Raspberry Pi computers that communicate with each other with Ethernet, WiFi, and the Robot Operating System (ROS) [21]. Each Raspberry Pi is a Model 4b with 8 GB of RAM. ROS packages for terrain mapping, local planning, localization, and manual teleoperation have been developed. The packages are divided among the four micro-controllers based on their computational needs.

The sensor suite consists of a stereo depth camera, a 2D lidar, and an inertial measurement unit (IMU).

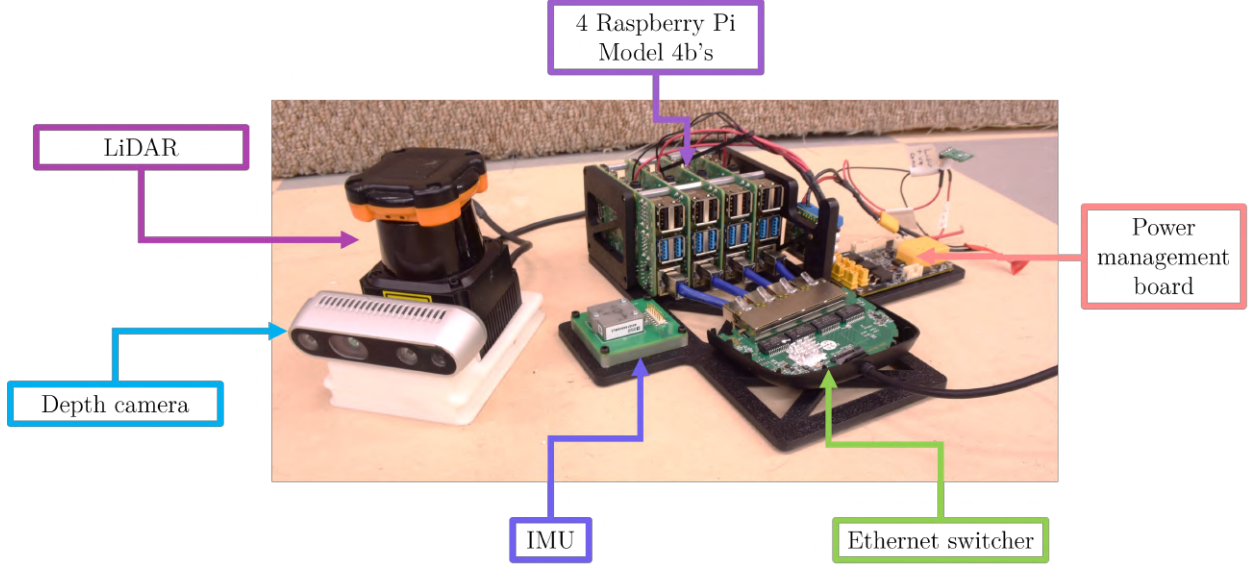


Figure 7: Sensor suite and electronics block for ET-Quad.

The depth camera and lidar are mounted on the exterior of the robot body at a small incline to better see the ground in front of ET-Quad. Currently, the external sensors are removed for swimming tests.

The onboard computers communicate with a base station computer with a WiFi network that can be hosted externally or from the base station. As all mapping and path planning is computed on ET-Quad, and it is capable of functioning with only intermittent communication with the base station computer, which provides high-level goal points and communicates with mission control. A communication diagram for ET-Quad is shown in Figure 8.

For in-lab development, a Vicon Motion Capture System was used for localization as this helped facilitate autonomy and locomotion tests. Field and lunar deployment will depend on visual and inertial odometry, as well as leg encoders, to perform simultaneous localization and mapping (SLAM) with the onboard computers. Localization in a lunar scenario could also make use of sensors and additional communication from the lunar base station.

4.3 Controls and Planning

ET-Quad implements a tiered controls approach. A high-level planner defines a path around obstacles that utilizes ET-Quad's various locomotion capabilities, and a low-level controller commands motor positions and velocities to achieve the correct gaits to carry out the plan.

4.3.1 Mapping and Terrain Generation

Before planning paths in the local environment, data is gathered about the surrounding terrain structure and potential obstacles that ET-Quad should avoid. This is done by using the lidar and RealSense Depth Camera data in unison to determine where the surfaces of the terrain lie and storing the data over time to fill in a $5\text{m} \times 5\text{m}$ local map. The data for the local map is stored in a multilayered structure using grid_map [22], allowing for convenient lookup and communication of terrain data via ROS.

The incoming data stream from the sensors undergoes processing before being passed to the planner, including ground classification, inpainting, radial blurring, and slope informed gait type prediction. This gives the planner more information about the environment and allows for more accurate trajectories to the goal point.

As indicated in Figure 9, ground classification of incoming data points is done by finding the plane (Π_g) that best fits a random sample of points between 0.5 and 1 meters in front of ET-Quad and using a set

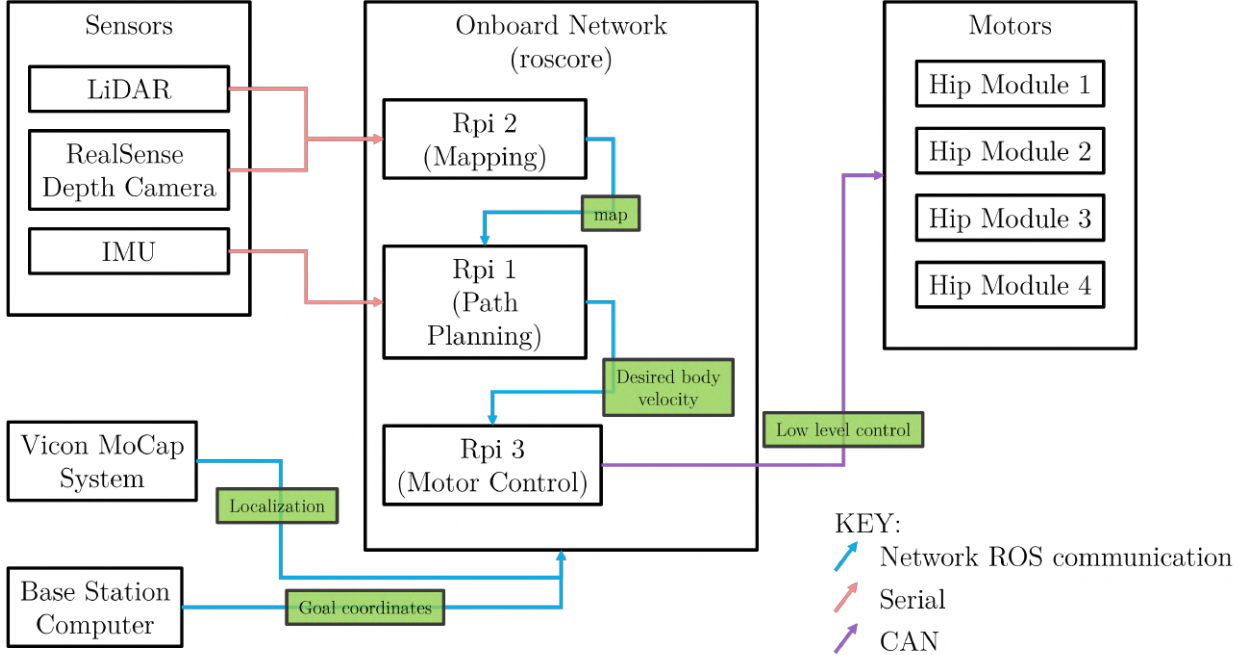


Figure 8: Communication diagram for ET-Quad. There are four Raspberry Pi Model 4b's onboard ET-Quad. One functions as a “master” and runs the ROScore. The other three are dedicated to mapping, planning, and motor control. The base station computer is intended to run on a lander or mobile rover during the lunar mission, and communicates with ET-Quad over a WiFi network. ET-Quad is capable of functioning with intermitent connections to the base station computer.

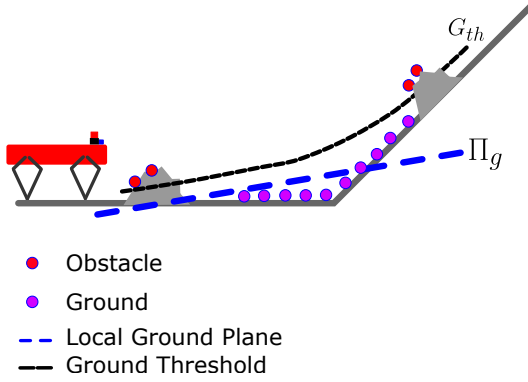


Figure 9: Classification of point cloud data into obstacles and ground based on parabolic ground threshold and ground plane estimation.

threshold distance away from that plane to classify the point as either ground or an obstacle. The threshold distance to the ground plane (G_{th}) increases parabolically with respect to distance from ET-Quad, and is used this way as the distinction between an obstacle and a climbable hill becomes less definitive the farther from the robot a point is. To minimize abrupt changes in the classification, a temporal low pass filter is employed.

4.3.2 High-Level Planning

We have developed a high-level planner for ET-Quad that uses a Sampling Based Model Predictive Optimization (SBMPO) framework [23]. Our approach uses a cost map based on obstacle data obtained from onboard sensors. In addition, we consider solar irradiance to generate energy optimal plans based on locomotion and temperature considerations. The planner employs a thermomechanical cost function that

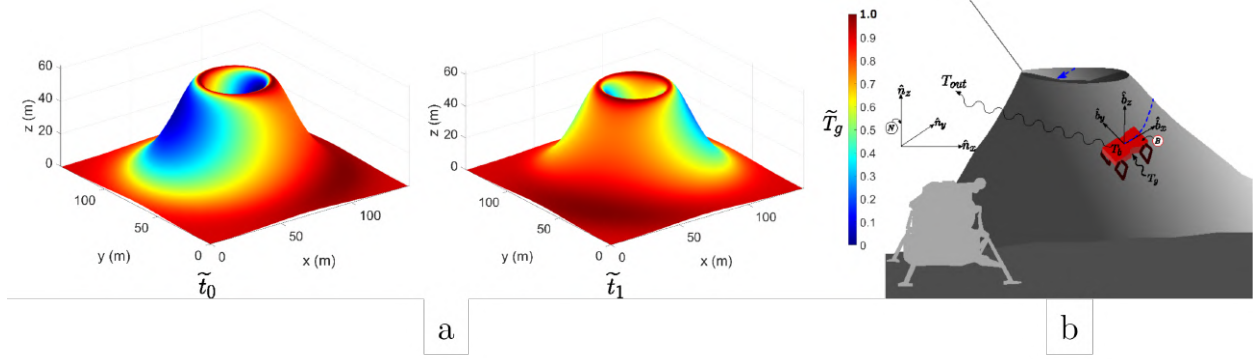


Figure 10: a) Normalized ground temperatures \tilde{T}_g at normalize times t_0 and t_1 . Times are normalized by the orbital period. b) ET-Quad robot ascending crater in an energetically efficient manner (dashed blue path). There is solar irradiance G and the robot body has temperature T_r . There are radiation effects with the ground at temperature T_g and outer space at temperature T_{out} . There is also heat conduction between the robot and the ground through its 4 legs. The inertial frame of reference is denoted by N , and the robot frame is B

includes radiation effects between the robot and the ground, the robot and outer space, and conduction between the robot legs and the ground. The cost function also captures mechanical costs associated with acceleration, deceleration, frictional drag, and changes in elevation [24].

Figure 10 illustrates an example of thermal maps with normalized ground temperatures \tilde{T}_g at two different normalized times \tilde{t}_0 and \tilde{t}_1 . Times are normalized by the orbital period.

When this thermal map is combined with a thermomechanical model of ET-Quad and the environment (outlined in Table 1), we are able to generate energy optimal trajectories to a goal point, as illustrated in Figure 10. This framework is the first time that we are aware of that thermal considerations have been implemented in a motion planning algorithm for a legged robot.

Table 1: Constants and thermophysical properties

Symbol	Variable	Value	Reference
G	Solar constant	1367 W/m ²	[25]
A	albedo	0.12	[26]
c_p	specific heat		
ρ	density	1100 kg/m ³	[27]
k	thermal conductivity		
ϵ	emissivity	0.95	[28]
P	lunar diurnal period	2.55×10^6 s	[29]

The same motion planning framework (SBMPO) is used by ET-Quad to avoid obstacles and plan routes that involve changes of gaits. For local navigation, ET-Quad considers local terrain in a $5\text{m} \times 5\text{m}$ environment.

4.3.3 Low-Level Control

ET-Quad executes the paths generated by the high-level planner with feed forward gaits designed for walking, climbing, and moving through resistive media. These gaits have been designed by hand with 500 points in the Cartesian workspace of ET-Quad’s feet that form a periodic cycle. These trajectories are then converted to motor positions using a geometric inverse kinematics formula. A proportional-derivative (PD) control law is used to follow the trajectories and create a stable gait.

Ongoing work in low-level control and path following includes transition gaits between different modes of locomotion (such as walking and climbing) and the development of robust and predictable turning gaits.

4.4 Technical Specifications

Here we outline high level technical specifications for ET-Quad, which will inform critical mission aspects such as transit to the moon and base station requirements.

4.4.1 Mechanical

ET-Quad has a total mass of 7.85 kg. The four hips and legs together have a mass of 3.8 kg, the batteries 0.40 kg, and the computation and electronics 0.85 kg.

ET-Quad fits in a bounding box of 0.07 m^3 when the legs are at nominal extension, with a width of 34 cm, height of 40 cm, and length of 52 cm.

The primary links of the 5-bar leg mechanisms are 66 mm long, and the secondary links are 180 mm long. The ratio of the lengths of these links is critical for energy efficient locomotion in various modes [12].

4.4.2 Electrical

ET-Quad operates at a nominal voltage of 28V, which is provided by two four-cell lithium-polymer batteries with 2800 mAh of charge each.

4.4.3 Computation & Communication

ET-Quad communicates with the base station via a local WiFi network. Consistent connection is only required for a remote operator to receive video feeds, if desired. The four internal Raspberry Pi model 4bs have 8 GB of RAM each and have Quad-core 64-bit processors that operate at 1.5 GHz. Internal communication between the Raspberry Pi's occurs via ethernet.

5 Verification testing on Earth

ET-Quad has been verified to exhibit its designed locomotion capabilities: walking on various terrains, climbing various slopes and substrates, and swimming through water which, like lunar regolith, we classify as a resistive media. This section describes the testbeds used to carry out the verification as well as the results of component and system level tests that verify ET-Quad's capabilities.

5.1 Testbeds

In addition to the ET-Quad robot, the FAMU-FSU team has designed and fabricated several new testbeds to verify various components of ET-Quad. These include a single and double-legged boom arm, a drag tank, and a lunar-like boulder for climbing.

The boom arm consists of a pole that is able to rotate freely about one end, tracing a circular track. The end of the pole allows for modular attachment of a single hip and leg assembly of ET-Quad or a double leg assembly. This allows us to test various locomotion capabilities quickly and repeatably without the full robot system. The boom arm in both the single and double legs configurations is shown in Figure 11, subfigures a and c.

We have also built a drag tank with a sliding rail where one or two hip assemblies can be attached. A pulley system connects one of ET-Quad's legs to a force plate and, when the tank is filled with water, we can calculate the drag properties of various fin attachments on a leg. The drag tank is shown in Figure 11b.

The climbing boulder was created by applying a grout and gravel mixture to a wire mesh and shaping the mesh and texturing the grout to generate a natural appearing texture. The same process is used to make pillars to support the desired climbing slope. A section of the boulder is shown in Figure 11d. Other sections are in development.

5.2 Component Level Testing

The individual components of ET-Quad have been thoroughly tested to ensure each will perform to design specifications and allow system level operation to proceed. Component level testing begins the return of the V-diagram level. The tests performed here are used to confirm that the targeted design specification are verified prior to full assembly.

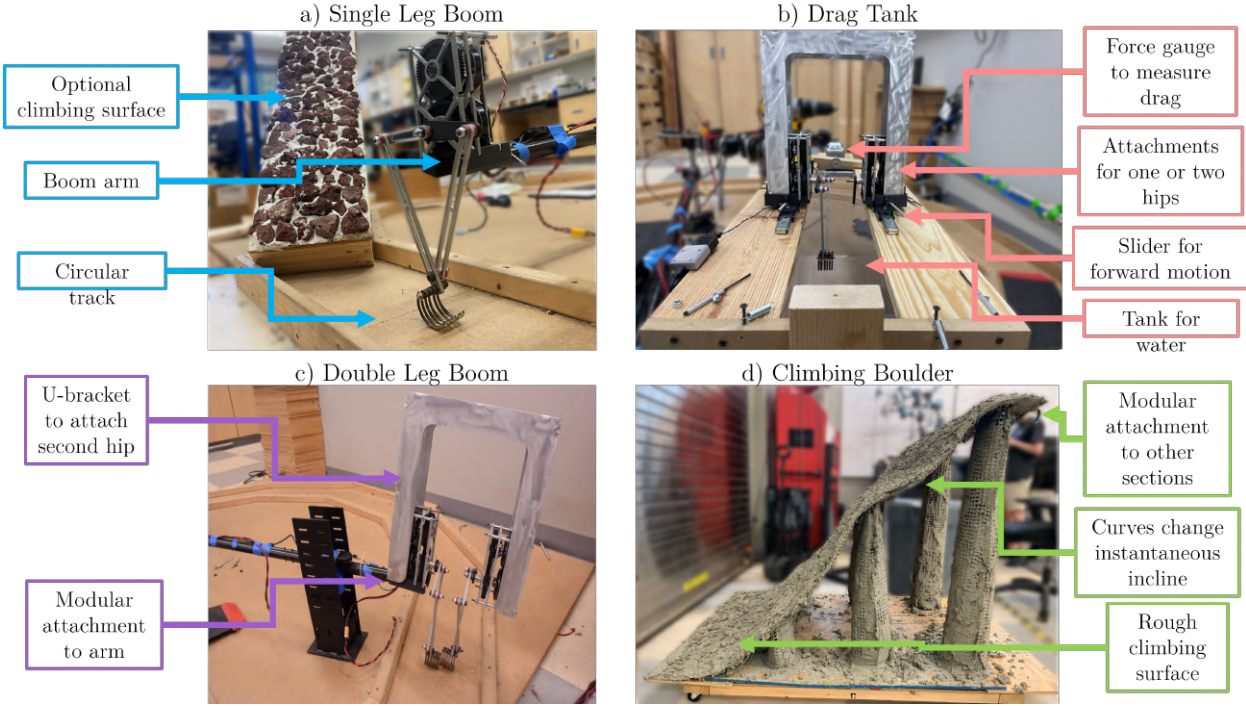


Figure 11: The various testbeds created to verify ET-Quad. a) A single legged boom for testing of legs and gaits. b) A drag tank for characterizing the drag properties of the legs and development of swimming gaits. c) A double legged boom for testing of leg coordination. d) A section of a climbing boulder for climbing on non-uniform surfaces.

5.2.1 Body Waterproofing

The robot body has been verified to be waterproof to approximately ISO 22810 standards. This was verified through splash, submersion, and waterjet testing on both the lid connection and the hip shafts. For splash testing, the body was placed under running water, and the water was allowed to drain away under the robot. The body was also submerged in shallow water for several seconds, and subjected to water jets from a hose.

5.2.2 Legs & Feet

The primary mechanical novelty of ET-Quad comes from the design of the legs and feet, which allow for autonomous multimodal locomotion. Consequently, these components have undergone extensive testing, which is described in this section.

Legs The fin prototypes discussed in Section 4.1.5 were tested to quantify drag properties for locomotion through resistive media. Torque data from the motors was taken while executing a swimming gait at 1.5 Hz for the leg moving through water with no attachments, a flap in the foot, a fin attached to the leg, and both the flap and the fin. The data from these tests are given in Table 2. The foot attachment was seen to oscillate and not be stiff enough to return to the correct position in order to contribute additional drag when the leg was run at a higher frequency. The increase in torque was also minimal when compared to the improvement using the side fins. Due to this, it was decided to use only the side fins when running full system swimming experiments.

Feet The feet of ET-Quad have been tested for traction, compliance, and climbing adhesion. Each of these characteristics are essential for successful locomotion in various modes.

Like legged animals, legged robots utilize mechanical compliance for energy efficient and robust locomotion [30, 31]. Consequently, the toes of ET-Quad were designed to compress and extend under loads. To test the stiffness of the toes, we clamped the end of the toe and pulled down, and then up, on the top of the toe with a mass spring scale. We then measured toe displacement and the required force. We were then able

Table 2: Torque on various leg attachments

	Peak torque (Nm)	ratio to no attachment
No attachment	0.240	1.0
Flaps on feet	0.265	1.10
Fin on leg	0.614	2.56
Flap and fin	0.642	2.67

to calculate a stiffness for a single toe and a whole foot. This process was repeated 10 times for individual toes and 10 times for a whole foot with rubber coating and with foam contact points. The results of these tests are given in Table 3.

Table 3: Results of stiffness tests for toes and feet

	Mean Stiffness in Compression (N/mm)	StDev Stiffness in compression	Mean Stiffness in Tension (N/mm)	StDev stiffness in tension
Single toe without foam	9.84	0.91	4.04	0.24
Single toe with foam	3.73	0.38	3.61	0.26
Full foot without foam	35.43	7.07	16.78	2.75
Full foot with foam	5.38	0.46	15.74	4.55

Successful walking relies on sufficient traction between the foot and a walking surface. To test the traction capabilities of various candidate rubber dips used on the bottom of the toes we placed a uniform piece of each rubber on a smooth plane of various surfaces. We then increased the angle of each plane and recorded the angle at which the piece of rubber started to slip down the plane. The tangent of this angle is the coefficient of friction between the two surfaces. The various coefficients of friction are given in Table 4.

Table 4: Coefficients of friction between various tested rubber coatings and various lab materials

	Abrasion resistant rubber	Impact resistant rubber	Corrosion resistant rubber
Smooth ABS	3.207	0.521	0.111
Steel	2.411	1.108	0.251
Wood	1.302	0.945	0.195
Smooth floor	3.833	1.401	0.864
Carpet	0.940	1.238	0.362
Rough floor	1.013	0.750	0.529
Rough ABS	1.591	1.043	0.502
High grit sandpaper	1.109	1.043	0.446
skateboard tape	1.109	1.955	1.003
Concrete	0.386	0.521	0.000

We have also tested climbing on the single leg boom to quantify attachment success. We recorded climbing at various angles and on various surfaces, including carpet, concrete, and garden lava rocks set in concrete (the lava rock wall is shown in Figure 11a). Each test was run for 10 climbing steps. The attachment success rate is recorded in Table 5.

5.2.3 Computation

The perception system updates on the Raspberry Pi 4b at an average rate of 150ms. The local planning with SBMPO on a 5 m×5 m map updates with average times of 22.1ms with an obstacle and 3.1 ms without obstacles. Global planning on 141 m×141 m maps ranges from 300-800 ms.

Table 5: Attachment success rate of the climbing feet at various angles on several surfaces

Angle ($^{\circ}$)	Attachment success on surface		
	Carpet	Concrete	Red Lava Rock
45	100%	100%	80%
55	90%	100%	70%
70	100%	100%	60%
85	100%	90%	-

5.2.4 Perception/Planning

As a test of the perception and planning system, the robot, as shown in Figure 12, is faced with an obstacle and a 60° hill. The robot perception system is able to successfully classify the terrain into traversable and nontraversable sections.

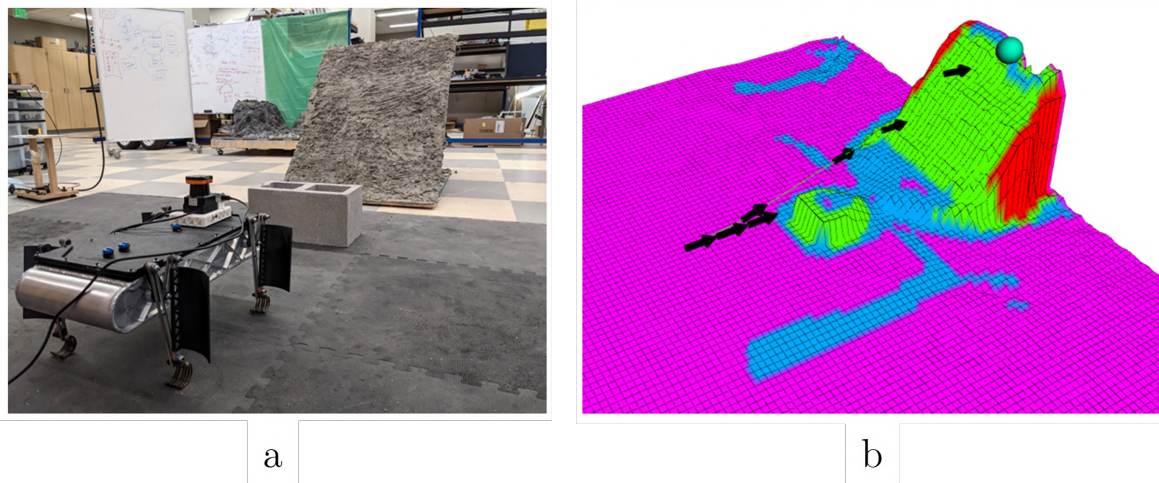


Figure 12: (a) ET-Quad facing an obstacle and a 60° hill (b) Resulting map showing elevation as well as desired gaits for each region. Purple represents a running gait, blue a walking gait, and green a climbing gait. A planned path to the goal at the top of the slope is also shown.

When the local maps are integrated with SBMPO, the robot is capable of planning motion that sequences its gaits. As indicated in Figure 12, the motion planner guides the robot by providing a sequence of high level commands (forward and angular velocities). The motion plan requires the robot to back up, proceed to walk around the obstacle, and finally transition to a climbing gait to overcome the steep incline and reach its local goal. The average computational time to plan this motion plan was 22.1ms.

At a global scale thermally informed motion planning was demonstrated in simulation in a terrain map of $141\text{m} \times 141\text{m}$. The terrain contains a crater like feature with varying ground temperatures in the range 200-400K. As shown in Fig. 13(a), the robot starts its mission on a cold region at $(x, y, \psi) = (20\text{m}, 122\text{m}, 5.49\text{rad})$ with a ground temperature of $T_g = 200\text{K}$. The goal of the robot is located inside the crater within the cold region ($T_g = 200\text{K}$) at $(x, y) = (65\text{m}, 65\text{m})$. The motion planner successfully finds a trajectory that takes the robot out of the cold ground early in the mission and proceeds towards the goal in the crater along more moderate temperatures. The plot shows a superposition of the ground temperature and the expansions (black dots) performed by SBMPO while optimizing the vehicle trajectory. The computational time to plan this trajectory was of 742.42ms.

In Figure 13(b), the robot starts its mission at $(x, y, \psi) = (122\text{m}, 20\text{m}, 2.36\text{rad})$ with a ground temperature of $T_g = 364.2\text{K}$. The goal of the robot is located inside the crater within the cold region at

$(x, y) = (65\text{m}, 65\text{m})$ and ground temperature $T_g = 200\text{K}$. The motion planner guides the robot and determines that an energetically efficient route to the goal by following the rim of the crater instead of taking a more direct route to the goal but with higher thermal cost. The computational time to plan this trajectory was of 367.42ms.

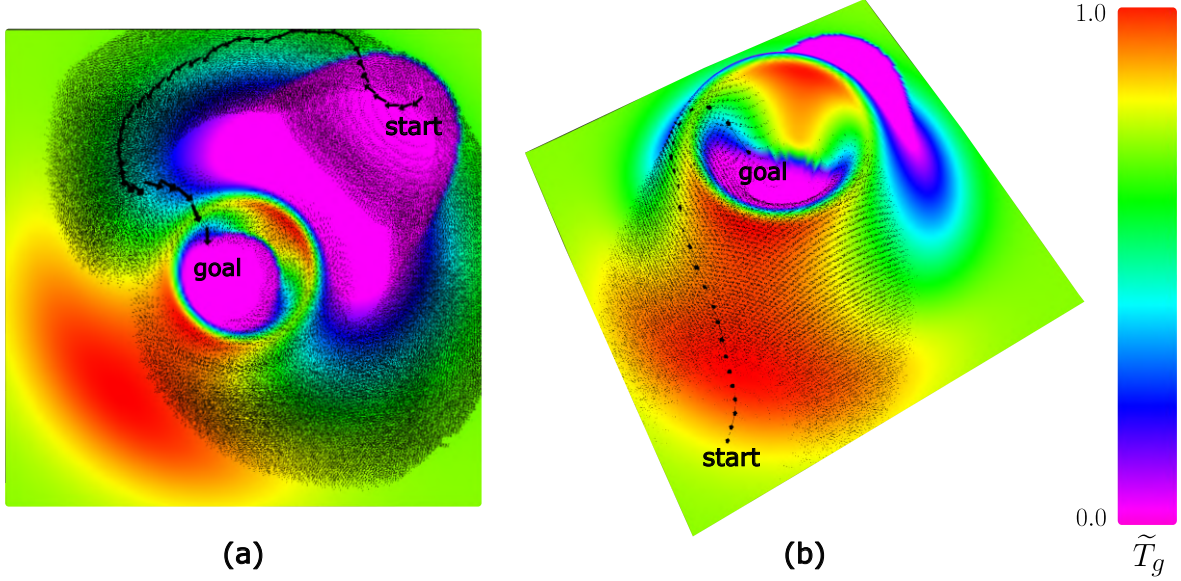


Figure 13: (a) Motion planning results with robot starting on a cold region $T_g = 200\text{K}$. (b) Motion planning results with robot starting on hot region $T_g = 364.2\text{K}$.

5.3 System Level Testing

With the component testing complete, the full ET-Quad system was verified for its locomotion capabilities: walking, climbing, and swimming through resistive media.

5.3.1 Walking

ET-Quad has demonstrated successful walking, as shown in the Verification Demonstration Video. We have found that walking with the manually designed gait is most robust on soft surfaces, such as the grass shown in the video, which will likely be an advantage for lunar locomotion. Increasing the robustness and reliability of the gait is an objective for ongoing testing and development.

Two walking frequencies were tested on grass: 2.5 Hz and 2.75 Hz. The slower gait, 2.5 Hz, consumed 44.2 mAh of battery charge over a 50 step test. The 2.75 Hz gait consumed 52.0 mAh of charge over 50 steps. At 2.75 Hz ET-Quad walks at approximately 25 cm s^{-1}

5.3.2 Climbing

ET-Quad's climbing capabilities were tested on a concrete surface prepared the same way as the boulder described in Section 5.1 and on a carpet wall with an adjustable slope previously installed at the FAMU-FSU College of Engineering. The manually designed climbing gait was tested on the carpet with an experimental sweep that covered angles between 60 and 90 degrees at a gait frequency of 0.5 Hz and gait frequencies between 0.5 Hz and 2.5 Hz at an incline of 70 degrees. On the concrete surface climbing frequencies of 0.5 Hz and 1.5 Hz were tested at angles of 45 and 60 degrees.

At low frequencies ET-Quad performed well at all tested angles on carpet and at 45 degrees on concrete. Climbing on carpet was successfully achieved at all frequencies up to 2.5 Hz at 70 degrees, and a limit of 1 Hz was discovered at 90 degrees. The maximum incline is lower for concrete, which indicates that successful climbing depends on reliable attachment.

The total electrical charge consumed for climbing ranged from approximately 25 mAh to 60 mAh for

a single 30 step test. Several examples of successful climbing are shown in the Verification Demonstration Video.

The speeds achieved while climbing ranged from 2.6 cm s^{-1} when climbing at a gait frequency of 0.5 Hz to 15 cm s^{-1} when climbing at 2.0 Hz.

5.3.3 Swimming

To verify ET-Quad's ability to traverse resistive media, we tested surface swimming in water deep enough to prevent the feet from touching the bottom, as seen in the Verification Demonstration Video.

While swimming on the surface of deep water, ET-Quad achieved a speed of 8.7 cm s^{-1} with a gait frequency of 1.5 Hz and a manually designed gait. The charge consumption was 9.53 mAh over 30 strides. This capability is shown in the Verification Demonstration Video.

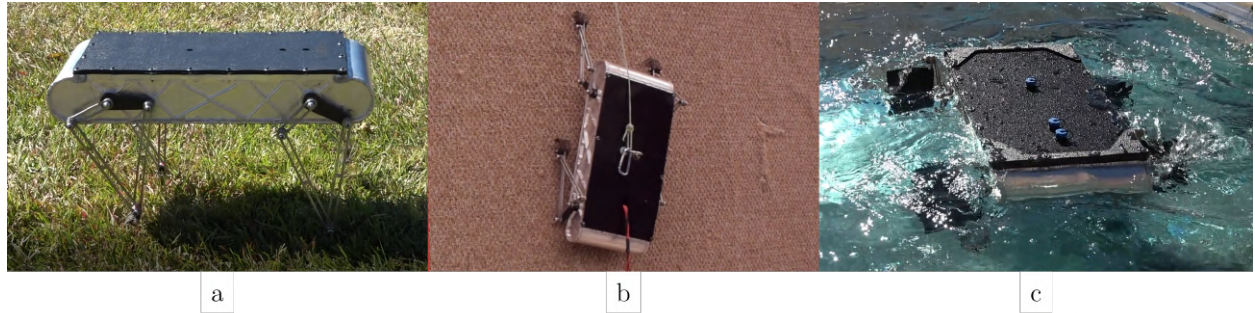


Figure 14: ET-Quad demonstrating its various locomotion modes: a) walking, b) climbing, and c) swimming.

6 Safety plan and protocols followed

Below is a relevant subset of the FAMU-FSU safety policy which was implemented during the ET-Quad project. An example is included in Table 6:

1. Laboratory workers performing research in FAMU-FSU are required to conduct a Project Hazard Assessment (PHA) to identify existing hazards and to determine proper measures to control those hazards.
2. The Primary Investigators (PI) must review, approve, and sign the written PHA.
3. The PI must ensure the control methods identified in PHA are implemented in the laboratory.
4. If laboratory personnel are not following the safety precautions, PI must take firm actions to clarify the safety expectations.
5. The PI must document all the incidents or accidents in the laboratory with the PHA document to ensure that PHA is reviewed or modified to prevent reoccurrence.
6. The PI must ensure that those findings in PHA are communicated with other students working in the same laboratory (affected users).
7. The PI must ensure that approved methods and precautions are being followed by: Performing periodic laboratory visits to prevent the development of unsafe practice; quickly reviewing the safety rules and precautions in the laboratory members meetings; Assigning a safety representative to assist in implementing the expectations.

7 Path-To-Flight

Here we describe aspects of the path to flight including plans for continued terrestrial development and platform modifications for extra-planetary deployment.

Table 6: Example of the Project Hazard Assessment

Experiment Steps	Location	Person assigned	Potential hazards/failures	Control Method	PPE	Waste Disposal	Residual Risk	Rules on residual risk
Connect Li-ion battery to charger	AME 123: CISCOR	Worker name	Leads are connection to battery first and able to shock worker	Leads are treated to charger	None	None	HAZARD: 2 CONSEQ: Low Med	Protocol instruction to be fixed to the charger's location

7.1 Continued Terrestrial Testing and Development

Continued development and testing of ET-Quad version 2 will improve its agility and functionality on more complex and challenging terrains. A few of the immediate plans for the robot include:

- Improve the leg designs for rough terrain traversal. For example, see Figure 15. The additional prongs on the tips of the feet work to improve walking by both increasing traction and as springs for a more compliant contact. The arched distal leg limb and spikes enable better attachment when climbing.
- Run experiments on regolith simulants to measure effectiveness of walking and swimming gaits in lunar-like environments.
- Develop and test transient behaviors as the robot moves from walking to swimming to climbing. New real-time optimal controllers will be developed for ET-Quad allowing it to approach a steep slope and then switch to a climb, or automatically adjust its walking gait to a swimming/trudging gait when encountering unexpected water, mud, or soft regolith.
- Integrate the sensors and software packages with the low-level controllers to enable online mapping and path planning and achieve fully autonomous navigation and obstacle avoidance.

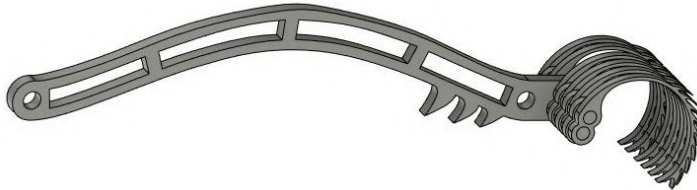


Figure 15: Updated all-metal leg foot design for improved attachment on rough terrain and more compliance when walking.

ET-Quad Version 3 We intend to continue to iterate on the ET-Quad design with the objectives of making the robot lighter, faster, and improving its range of mobility in different environments. This new version will exchange the motors and with a smaller, frameless, hollow-bore motors that can be run with moderate gearing to maintain the low impedance and the concentric-coaxial shaft design. These will be run with the new o-drive motor controller. With smaller more power dense actuators, the body will be shrunk and some sensors will be replaced including the lidar (with the new Velobit) to minimize weight. The new, lighter design will allow for increased speed of locomotion and make a wider range of climbing surfaces accessible without substrate failure. Furthermore, a third, out-of-plane degree of freedom per leg will be explored (with a design focus on waterproofing) to enable more complex maneuvers. Each of these features will enable ET-Quad to maneuver with greater flexibility on a variety of terrain challenges under Earth’s gravitational conditions.

Model Based Systems Engineering (MBSE) As the project developed, the team found silos of engineering that proved to challenge progress. For example, software such as MATLAB, Simulink, and Simscape are all compatible as they are all manufactured by MathWorks, but the integration between the software requires a call function to the most current model, which assumes the called file is the most accurate model. Further,

the geometric integration, bill of materials, and additive manufacturing software were all different from MATLAB and from each other. Recognizing these silos has spawned an undergraduate senior Capstone Design project to address the MBSE needs from ET-Quad (and other quadrupedal robots). The continued development is looking at methods of project data management, system requirement management, parametric design, and sensitive design variables, in order to provide the highest impact on designs. This effort should minimize rework, catch errors early, and improve communication. The continued work should create architectures that are more flexible and communicate needs and changes across software platforms. The MBSE approach will optimize design through more and faster trade studies.

7.2 Modifications for Extra-planetary Deployment

While ET-Quad was designed for terrestrial operation, several aspects of the robot have already been designed in preparation for a lunar mission, these include the aluminum body for dust penetration and basic electro-magnetic shielding, the compliant steel claws for walking and climbing modes, and a sensor suite with update speeds sufficient for local mapping at lunar speeds. The following are some key areas that will need updating prior to fielding.

Dust Management While insulated against water penetration, the body and legs will need upgrades to deal with the accumulation of abrasive regolith. Possible steps include adding isolating caps on the joints, flexible sheaths for the legs, or electronically generated fields to repel dust buildup on the legs. Proper testing in regolith simulants will need to be done to determine what combination of these methods will provide the best protection for the legs.

Control Adaptations The reduced lunar gravity has several benefits for the tasks of legged locomotion including reducing leg torque requirement and impact loading, but changing gravity will necessitate motor selection and control modifications. Simulations and dynamic scaling should allow us to estimate new control policies and efficiency estimates (e.g. we estimate that foot forces will be reduced by a factor of 0.165 and the stride frequencies reduced by 0.407).

Power Source For extended operation in space, ET-Quad's power supply mechanism will need to be updated. Possible solutions may include recent advances in solid state batteries, multi-mission radioisotope thermoelectric generators (MMRTG) and/or solar cells. In any case, the power supply will need to remain small in order to fit on the robot while still generating the baseline power for the locomotion requirements.

Thermal Regulation Given the low temperatures expected on the moon, internal heating (rather than cooling) will be a major consideration in a flight-ready version of ET-Quad. Some of the energy from the updated power source will be needed to be used to maintain working internal temperatures, which may make the MMRTG a good candidate for this task. In particular, active thermal conductivity will need to be present on the actuator mounts and on the intelligence stack, perhaps with additional material insulation on the body and around critical components.

8 Results and Conclusions

The objective of this project was to demonstrate an alternative lunar mobility solution: a legged robot capable of exploration and delivery of small payloads in unstructured lunar-like environments such as steep slopes, rocky terrain, and resistive media, such as high-porosity regolith. To this end we developed ET-Quad, a small, lightweight robot capable of walking, climbing steep slopes (up to vertical on a prepared surface), and swimming through resistive media (in our case water). To our knowledge, this is the first legged robot designed to move in all three domains.

Particular accomplishments include:

- Developed novel feet and legs for tri-modal locomotion. Independently-compliant spines allow for improved attachment on rough, rocky surfaces when climbing. The parallel structure and curved shape of the foot allows for different functional stiffness for walking on rigid substrates. Directionally-

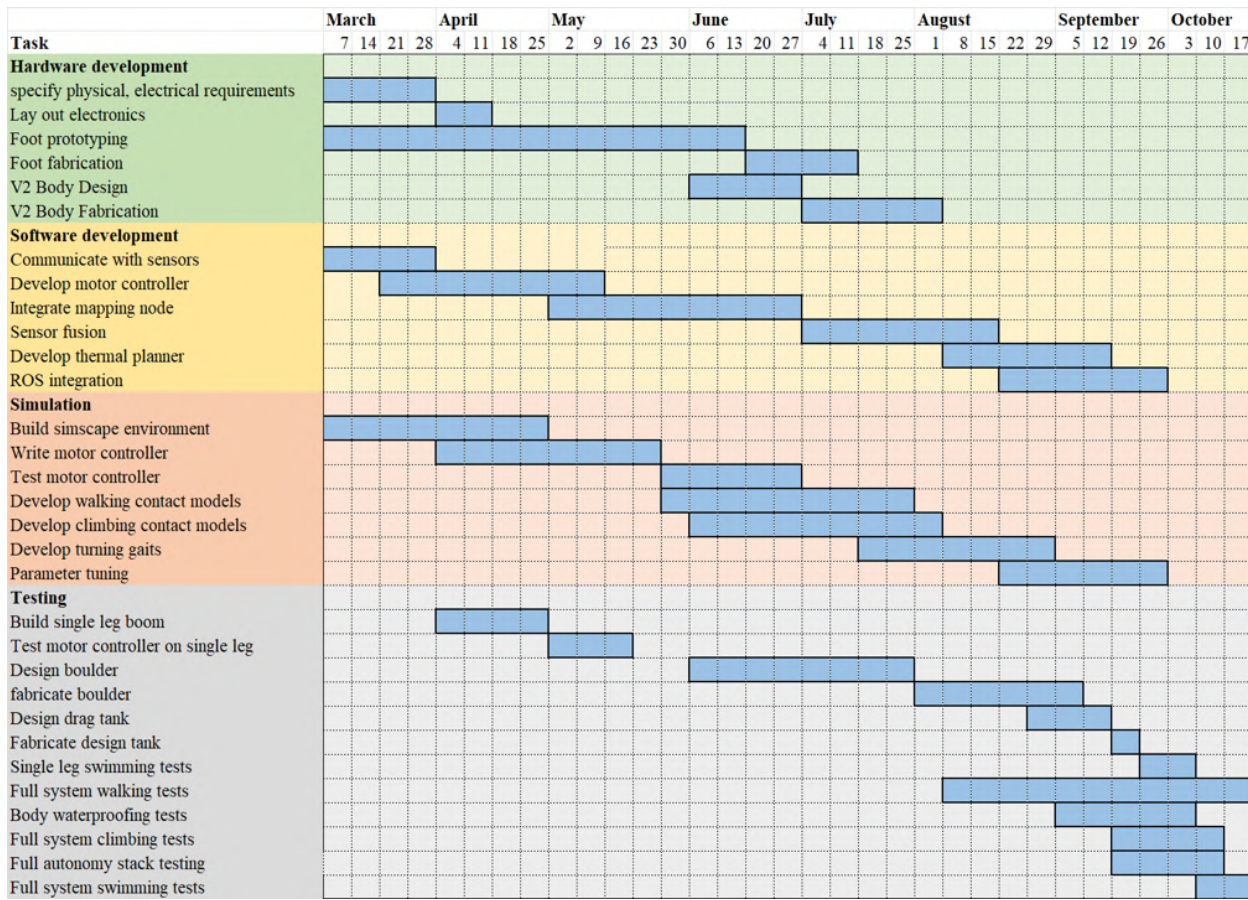
compliant fins allow for improved drag characteristics when moving through resistive media, such as water.

- Developed a light-weight autonomy perception and intelligence stack for real-time obstacle identification, avoidance, and mode-transitions. Of note, this planner creates a 3D map that includes climbable regions, and can choose the correct gait based on terrain characteristics.
- Developed a novel thermally-informed, real-time motion planning algorithm to allow a rover to avoid time-varying cold regions during operation.

We note that by having the walking, climbing, and swimming integrate through the legs, the complexity of systems is reduced and the amount of single-function parts is minimized. There are no parts of the robot, such as a propeller, that only contribute to a single mode.

The multi-modal capabilities of this platform open up a host of exciting potential research questions, such as how to construct modal transition behaviors, select optimally efficient multi-domain paths, and develop terrain-adaptive controllers. These advances will lead to more versatile and robust rovers on extra-terrestrial bodies, and a better understanding of locomotion (both robotic and animal) here on Earth.

9 Timeline



10 Budget

Description	Phase 1 1/1/22-6/30/22		Phase 2 7/1/2022-11/30/22			Overall	
	Budget	Actual	Budget	Actual	Encumbered	Budgeted	Actual
Materials							
Motors & Control	\$ 12,700.00	\$ 5,784.38	\$ 320.00	\$ 2,826.47			
Sensors & Computation	\$ 3,400.00	\$ 2,177.32	\$ 600.00	\$ 1,461.20			
Laptop	\$ 1,049.00	\$ 1,681.30	\$ 800.00	\$ 1,919.56			
Mechanical Hardware	\$ 751.00	\$ 1,041.22					
Fabrication	\$ 2,100.00	\$ 2,395.46	\$ 3,280.00	\$ 591.35			
Materials Subtotal	\$ 20,000.00	\$ 13,079.68	\$ 5,000.00	\$ 6,798.58		\$ 25,000.00	\$ 19,878.26
Labor							
Undergraduate Labor	\$ 14,080.00	\$ 12,739.28	\$ 12,320.00	\$ 10,067.44	\$ 13,486.08		
Graduate Labor	\$ 18,775.07	\$ 20,631.07	\$ 20,699.56	\$ 9,308.58	\$ 10,483.96		
Faculty Labor	\$ -		\$ 5,924.20	\$ 5,916.69			
Labor Subtotal	\$ 32,855.07	\$ 33,370.35	\$ 38,943.76	\$ 25,292.71	\$ 23,970.04	\$ 71,798.83	\$ 82,633.10
Travel							
Registration	\$ -	\$ -	\$ 4,400.00	\$ 2,750.00			
Airfare	\$ -	\$ -	\$ 4,000.00	\$ 3,958.00	\$ 2,600.00		
Lodging	\$ -	\$ -	\$ 4,320.00	\$ 2,515.97			
Meals & Incidental expenses	\$ -	\$ -	\$ 1,296.00		\$ 1,296.00		
Ground transportation	\$ -	\$ -	\$ 240.00		\$ 240.00		
Travel Subtotal	\$ -	\$ -	\$ 14,256.00	\$ 9,223.97	\$ 4,136.00	\$ 14,256.00	\$ 13,359.97
Indirect Costs							
University Indirect Costs	\$ 28,541.74	\$ 28,541.74	\$ 31,427.87	\$ 7,285.00			
Space Grant Indirect Costs			\$ 5,819.98	\$ -			
Indirect Costs Subtotal	\$ 28,541.74	\$ 28,541.74	\$ 37,247.85	\$ 7,285.00		\$ 65,789.59	\$ 35,826.74
TOTAL	\$ 81,396.81	\$ 74,991.77	\$ 95,447.61	\$ 48,600.26	\$ 28,106.04	\$ 176,844.42	\$ 151,698.07

References

- [1] A. Parness, N. Abcouwer, C. Fuller, N. Wiltsie, J. Nash, and B. Kennedy, “Lemur 3: A limbed climbing robot for extreme terrain mobility in space,” in *2017 IEEE International Conference on Robotics and Automation (ICRA)*. IEEE, 2017, pp. 5467–5473.
- [2] A. Bouman, M. F. Ginting, N. Alatur, M. Palieri, D. D. Fan, T. Touma, T. Pailevanian, S.-K. Kim, K. Otsu, J. Burdick *et al.*, “Autonomous spot: Long-range autonomous exploration of extreme environments with legged locomotion,” in *2020 IEEE/RSJ International Conference on Intelligent Robots and Systems (IROS)*. IEEE, 2020, pp. 2518–2525.
- [3] J. Stopar, M. Robinson, E. Speyerer, K. Burns, H. Gengl, and L. Team, “Regolith characterization using lroc nac digital elevation models of small lunar craters,” in *Lunar and Planetary Science Conference*, no. 1659, 2012, p. 2729.
- [4] T. Krüger, C. van Der Bogert, and H. Hiesinger, “Geomorphologic mapping of the lunar crater tycho and its impact melt deposits,” *Icarus*, vol. 273, pp. 164–181, 2016.
- [5] B. C. Roberts, “Cross-program design specification for natural environments (dsne),” vol. Revision H, 2020.
- [6] B. Thomson, P. Spudis, P. Hayne, J. Cahill, G. Patterson, C. Neish, T. Thompson, E. Heggy, and A. Stickle, “Evidence for possible low-density regolith at the lunar poles,” in *Lunar and Planetary Science Conference*, no. 1903, 2016, p. 2426.
- [7] S. Shrivastava, A. Karsai, Y. O. Aydin, R. Pettinger, W. Bluethmann, R. O. Ambrose, and D. I. Goldman, “Material remodeling and unconventional gaits facilitate locomotion of a robophysical rover over granular terrain,” *Science Robotics*, vol. 5, no. 42, 2020.
- [8] J. D. Dickson and J. E. Clark, “Design of a multimodal climbing and gliding robotic platform,” *IEEE/ASME Transactions on Mechatronics*, vol. 18, no. 2, p. 494–505, 2013.
- [9] J. M. Brown, M. P. Austin, B. D. Miller, and J. E. Clark, “Evidence for multiple dynamic climbing gait families,” *Bioinspiration & biomimetics*, vol. 14, no. 3, p. 036001, 2019.
- [10] M. Austin, J. Nicholson, J. White, S. Gart, J. Pusey, C. Hubicki, and J. Clark, “Optimizing dynamic legged locomotion in mixed, resistive media (under review),” in *2022 IEEE International Conference on Robotics and Automation (ICRA)*. IEEE, 2022.
- [11] R. Alicea, K. Ladyko, and J. Clark, “Lift your leg: Mechanics of running through fluids,” in *2019 International Conference on Robotics and Automation (ICRA)*. IEEE, 2019, pp. 7455–7461.
- [12] M. P. Austin, J. M. Brown, C. A. Young, and J. E. Clark, “Leg design to enable dynamic running and climbing on bobcat,” in *2018 IEEE/RSJ International Conference on Intelligent Robots and Systems (IROS)*. IEEE, 2018, pp. 3799–3806.
- [13] G. E. Dieter and L. C. Schmidt, *Engineering Design*. McGraw-Hill, 2013.
- [14] M. P. Austin, J. M. Brown, C. A. Young, and J. E. Clark, “Leg design to enable dynamic running and climbing on bobcat,” in *Intelligent Robots and Systems (IROS), 2018 IEEE/RSJ International Conference on*. IEEE, 2018.

- [15] J. Nicholson, J. Jasper, A. Kourchians, G. McCutcheon, M. Austin, M. Gonzalez, J. Pusey, S. Karumanchi, C. Hubicki, and J. Clark, “Llama: Design and control of an omnidirectional human mission scale quadrupedal robot,” in *2020 IEEE/RSJ International Conference on Intelligent Robots and Systems (IROS)*. IEEE, 2020, pp. 3951–3958.
- [16] R. Blickhan, “The spring-mass model for running and hopping,” *Journal of biomechanics*, vol. 22, no. 11-12, pp. 1217–1227, 1989.
- [17] D. I. Goldman, T. S. Chen, D. M. Dudek, and R. J. Full, “Dynamics of rapid vertical climbing in cockroaches reveals a template,” *Journal of Experimental Biology*, vol. 209, no. 15, pp. 2990–3000, 2006.
- [18] D. J. Blackman, J. V. Nicholson, C. Ordóñez, B. D. Miller, and J. E. Clark, “Gait development on minitaur, a direct drive quadrupedal robot,” in *SPIE Defense+ Security*. International Society for Optics and Photonics, 2016, pp. 98370I–98370I.
- [19] B. D. Miller, “Dynamic legged robots for use in multiple regimes: Scaling, characterization and design for multi-modal robotic platforms,” Ph.D. dissertation, The Florida State University, 2013.
- [20] M. Spenko, G. C. Haynes, J. Saunders, M. R. Cutkosky, A. A. Rizzi, R. J. Full, and D. E. Koditschek, “Biologically inspired climbing with a hexapedal robot,” *Journal of Field Robotics*, vol. 25, no. 4-5, pp. 223–242, 2008.
- [21] Stanford Artificial Intelligence Laboratory et al., “Robotic operating system.” [Online]. Available: <https://www.ros.org>
- [22] P. Fankhauser and M. Hutter, “A Universal Grid Map Library: Implementation and Use Case for Rough Terrain Navigation,” in *Robot Operating System (ROS) – The Complete Reference (Volume 1)*, A. Koubaa, Ed. Springer, 2016, ch. 5. [Online]. Available: <http://www.springer.com/de/book/9783319260525>
- [23] M. Harper, C. Ordóñez, and E. Collins, “Sbmpo: Sampling based model predictive optimization for robot trajectory planning,” *Software Impacts*, vol. 10, p. 100159, 2021.
- [24] C. Ordóñez, J. Ordóñez, J. Boylan, J. Lupton, D. Vazquez, and J. Clark, “Thermally informed motion planning to enhance mission endurance of mobile robots,” in *8th Thermal and Fluids Engineering Conference (TFEC)*, 2023 (under review).
- [25] A. V. Da Rosa and J. C. Ordóñez, *Fundamentals of renewable energy processes*. Academic Press, 2021.
- [26] A. R. Vasavada, J. L. Bandfield, B. T. Greenhagen, P. O. Hayne, M. A. Siegler, J.-P. Williams, and D. A. Paige, “Lunar equatorial surface temperatures and regolith properties from the diviner lunar radiometer experiment,” *Journal of Geophysical Research: Planets*, vol. 117, no. E12, 2012.
- [27] W. D. Carrier III, G. R. Olhoeft, and W. Mendell, “Physical properties of the lunar surface,” *Lunar sourcebook*, pp. 475–594, 1991.
- [28] L. M. Logan, G. R. Hunt, S. R. Balsamo, and J. W. Salisbury, “Midinfrared emission spectra of apollo 14 and 15 soils and remote compositional mapping of the moon,” in *Lunar and Planetary Science Conference Proceedings*, vol. 3, 1972, p. 3069.
- [29] K. R. Lang, *Astrophysical data: Planets and stars*. Springer Science & Business Media, 2012.

- [30] M. Raibert, *Legged Robots that Balance*, ser. Artificial Intelligence. MIT Press, 1986. [Online]. Available: <https://books.google.com/books?id=EXRiBnQ37RwC>
- [31] R. M. Alexander, *Principles of animal locomotion*. Princeton University Press, 2003.